(2)

MTL TR 89-61

AD

CORROSION AND CORROSION INHIBITION OF METALS/ALLOYS IN METHYLPHOSPHONIC DIFLUORIDE AND DECONTAMINATING SOLUTIONS

CHESTER V. ZABIELSKI, MILTON LEVY, and
JAMES SCANLON
METALS RESEARCH BRANCH

July 1989

Approved for public release; distribution unlimited.

US ARMY
LABORATORY COMMAND
MATERIALS TECHNOLOGY LABORATORY

Sponsored by
U.S. Army Chemical Research, Development
and Engineering Center
Aberdeen Proving Ground, Maryland

U.S. ARMY MATERIALS TECHNOLOGY LABORATORY
Watertown, Massachusetts 02172-0001

The findings in this report are not to be construed as an official Department of the Army position, unless so designated by other authorized documents.

Mention of any trade names or manufacturers in this report shall not be construed as advertising nor as an official indorsement or approval of such products or companies by the United States Government.

DISPOSITION INSTRUCTIONS

Destroy this report when it is no longer needed.
Do not return it to the originator.

UNCLASSIFIED

SECURITY CLASSIFICATION OF THIS PAGE (*When Data Entered*)

REPORT DOCUMENTATION PAGE		READ INSTRUCTIONS BEFORE COMPLETING FORM
1. REPORT NUMBER MTL TR 89-61	2. GOVT ACCESSION NO.	3. RECIPIENT'S CATALOG NUMBER
4. TITLE (*and Subtitle*) CORROSION AND CORROSION INHIBITION OF METALS/ ALLOYS IN METHYLPHOSPHONIC DIFLUORIDE AND DECONTAMINATING SOLUTIONS		5. TYPE OF REPORT & PERIOD COVERED Final Report 6. PERFORMING ORG. REPORT NUMBER
7. AUTHOR(*s*) Chester V. Zabielski, Milton Levy, and James Scanlon		8. CONTRACT OR GRANT NUMBER(*s*)
9. PERFORMING ORGANIZATION NAME AND ADDRESS U.S. Army Materials Technology Laboratory Watertown, Massachusetts 02172-0001 SLCMT-EMM		10. PROGRAM ELEMENT, PROJECT, TASK AREA & WORK UNIT NUMBERS
11. CONTROLLING OFFICE NAME AND ADDRESS U.S. Army Chemical Research, Development and Engineering Center Aberdeen Proving Ground, MD 21010-5423		12. REPORT DATE July 1989 13. NUMBER OF PAGES 20
14. MONITORING AGENCY NAME & ADDRESS (*if different from Controlling Office*)		15. SECURITY CLASS. (*of this report*) Unclassified 15a. DECLASSIFICATION/DOWNGRADING SCHEDULE

16. DISTRIBUTION STATEMENT (*of this Report*)

Approved for public release; distribution unlimited.

17. DISTRIBUTION STATEMENT (*of the abstract entered in Block 20, if different from Report*)

18. SUPPLEMENTARY NOTES

Presented at the 1988 U.S. Army Chemical Research, Development and Engineering Center Scientific Conference on Chemical Defense Research, held 15-18 November 1988 at the Conference Center, Edgewood Area, APG, MD and to be published in the Conference Proceedings.

19. KEY WORDS (*Continue on reverse side if necessary and identify by block number*)

Corrosion-resistant alloys
Corrosion inhibition
Decontamination materials
Methylphosphonic difluoride

20. ABSTRACT (*Continue on reverse side if necessary and identify by block number*)

(SEE REVERSE SIDE)

DD FORM 1 JAN 73 1473 EDITION OF 1 NOV 65 IS OBSOLETE

UNCLASSIFIED

SECURITY CLASSIFICATION OF THIS PAGE (*When Data Entered*)

Block No. 20

ABSTRACT

Electrochemical potentiodynamic polarization studies have been carried out for a variety of ferrous and nonferrous metals in methylphosphonic difluoride. Studies of the effect of organic inhibitors on the corrosion rate of 1020 steel, 316 and 304 stainless steel and magnesium in methylphosphonic difluoride were also carried out. In addition, electrochemical studies were conducted in Decon solutions of sodium carbonate, DS2, and STB. General corrosion rates are reported for ferrous alloys, titanium, aluminum alloys, magnesium, and two metal-matrix composites in full strength and diluted Decon solutions.

CONTENTS

INTRODUCTION

Binary munitions in which two different constituents are kept in separate compartments until activation will constitute a significant fraction of the chemical weapons in the United States. Because these munitions will be used under extreme circumstances, they must be stockpiled over very long periods of time (up to 30 years) and still be able to operate reliably when the need arises. A very high reliability of the storage container is essential to the subsequent activation of, and availability of, this weapon system. The failure of the storage container is a hazard in itself because of the toxic nature of one of the constituents. The principal cause of failure will be the corrosion of the storage container by the highly corrosive methylphosphonic difluoride (DF). This compound will react with alcohol in the weapon system to form the active agent (GB). The hydroscopic DF interacts with the minor amounts of water which may be present to form hydrogen fluoride (HF). DF is not used in pure form but contains significant amounts of chlorides and cathodic impurities such as iron, copper, and nickel which further increase the corrosion rate of most metals/alloys. Although polymeric liners are being used, they may slowly interact with HF in the DF, and the substrate metal/alloy must be able, therefore, to withstand corrosion and pitting attack. Pitting attack could lead to rapid perforation of the container. Vapor phase (thin electrolyte film) corrosion has been shown to be the primary failure mode in GB munitions, and is prevalent in DF systems. DF is a major constituent of GB. Electrochemical studies for metals/alloys in methylphosphonic difluoride were initiated under a joint MTL-CRDEC program.

Army weapons systems equipment may also be exposed to toxic chemical environments during their life cycle. When exposed, these systems must be decontaminated with solutions which neutralize toxic agents either by oxidation or by hydrolysis, but are highly caustic and may cause residual change.

The objectives of this study are: to investigate the kinetics and mechanisms of corrosion of Al 6061-T6 and candidate metal alloys in methylphosphonic difluoride (DF), to establish effective corrosion inhibitors and tc ultimately incorporate or immobilize inhibitors into coatings which can provide protection above the liquid line, and to determine the corrosion rates and behavior of selected metals/alloys and metal-matrix composites in decontaminating solutions.

EXPERIMENTAL

Materials

DF Study: The DF was utilized in two purities, 97.1% and 99.8%. The complete compositions are shown in Table 1. Potential organic inhibitor materials were added to DF to determine their effects on the corrosion processes and to provide a means for protecting the alloys against corrosion. A variety of metals/alloys were utilized. Nominal compositions for the ferrous and nonferrous metals/alloys are contained in Tables 2 through 6.

Table 1. ANALYSIS AND PURITY OF DF

Analysis	Samples	
	DF-2	DF-22*
Metals (ppm)		
Fe	120	7
Cu	10	10
Ni	18	22
Cr	4	1
Zn	18	2
Mo	2	2
Total Metals (wt%)	0.017	0.004
Cl (wt%)	0.22	0.01
Purity (mole % by method:)		
FP Depression	97.1	99.8
NMR	96.8	99.9
Impurities (mole %)		
Percent Accountable	0.237	0.0014
Percent Not Accountable	2.763	0.249

*Represents DF purified by distillation in Hastelloy B equipment to produce high-purity material

Table 2. COMPOSITION OF NONFERROUS ALLOYS

Alloy	Nominal Composition (wt%)				
	Ta	W	Ti	U	Mg
Pure Ta	99.9	–	–	–	–
Ta-10W	90	10	–	–	–
PureTi	–	–	99.9	–	–
Pure Mg	–	–	–	–	99.9
U-0.75%Ti	–	–	0.75	99.25	–

Table 3. COMPOSITION OF STAINLESS STEEL ALLOYS

Alloy	Nominal Composition (wt%)						
	Fe	Ni	Cr	Mn	Mo	Si	Cu
20Cb3	35	35	20	2	2.5	1	3.5
317L SS	60	12	19	2	3.5	1	–
316L SS	65	12	17	2	2.5	1	–
304 SS	68	10	19	2	–	–	–
430 SS	80	0.8	17	1	–	1	–
1020	99	–	–	0.5	–	–	–

Table 4. COMPOSITION OF NICKEL ALLOYS

Alloy	Nominal Composition (wt%)					
	Ni	Cr	Mo	Fe	Cu	W
Hast. C	59	16	16	5	–	4
Hast. B	61.2	1	28	5	–	–
Monel	66.5	1.3	–	–	31.5	–
Ni 200	99.5	–	–	–	–	–
Pure Ni	99.9	–	–	–	–	–

Table 5. COMPOSITION OF ALUMINUM ALLOYS

Alloy	Nominal Composition (wt%)							
	Al	Si	Mg	Cu	Fe	Mn	Zn	Li
Al 2017	93	0.6	0.6	4	0.7	0.7	–	–
Al 2090	93.4	–	–	2.8	–	0.8	–	2.4
Al 4043	93	5.3	–	–	0.8	–	–	–
Al 5083	93	0.5	4.5	–	0.5	0.7	–	–
Al 6061-T6	97	0.6	1	–	0.7	–	–	–
Al 7075-T6	90	0.5	2.5	1.6	0.5	–	5.6	–

Table 6. COMPOSITION OF COPPER ALLOYS

Alloy	Nominal Composition (wt%)			
	Cu	Zn	Ni	Pb
Cu (38% Zn, 2% Pb)	60	38	–	2
Cu (30% Zn)	70	30	–	–
Gilding Metal	95	5	–	–
Pure Cu	99.9	–	–	–

Decon Study: The compatibility of three decontamination solutions: sodium carbonate, DS2 (an organic/hydroxide solution), and supertropical bleach (STB) with alloys of titanium, aluminum, and magnesium as well as several steels and metal-matrix composites of aluminum/SiC and magnesium/Al_2O_3 were assessed. Decontamination solutions and alloy compositions are shown in Tables 7 and 8.

Table 7. DECONTAMINATION SOLUTION COMPOSITIONS

Sodium Carbonate - 10 wt% Solution in Water	
DS2 -	70 wt% Diethylenetriamine 28 wt% Methyl Cellosolve (Ethylene Glycol Monomethyl Ether) 2 wt% Sodium Hydroxide
STB -	Calcium Hypochlorite Calcium Oxide - Added as a Stabilizer Water - Optional; Used to Form a Slurry

Table 8. SPECIMEN COMPOSITION DATA

Alloy	Density (gm/cm^3)	Equivalent Weight	Composition (wt%)
C 1020	7.86	28.98	C-0.17, Mn-0.42, P-0.009, S-0.006
20Cb3	7.86	24.53	C-0.019, Mn-0.34, Si-0.40, P-0.021, S-0.002, Cr-19.40, Ni-32.91, Mo-2.22, Cu-3.26, Cb + Ta-0.58
Ti-6Al-4V	4.43	11.70	C-0.02, Ni-0.014, Fe-0.14, Al-6.0, V-3.9, O-0.132
Al 5083-H112	2.66	9.18	Si-0.40, Fe-0.4, Cu-0.10, Mn-0.40/1.0, Mg-4.0/4.9, Cr-0.05/0.25, Zn-0.25, Ti-0.15
Al 6061-T6	2.70	9.15	Si-0.60, Cu-0.10, Mn-0.75, Mg-0.10, Cr-0.20, Zn-0.125
Al 7039	2.70	10.01	Cr-0.16/0.25, Cu-0.10, Fe-0.4, Mg-2.3/3.3, Mn-0.10/0.40, Si-0.30, Ti-0.10, Zn-3.5/4.5
Mg ZE41A	1.85	13.33	Zn-0.04, Ce-0.012, Zr-0.007
Al 2090			Cu-3.0, Li-2.6, Zr-0.15
Al MML 043			Cu-6.1, Li-1.3, Zr-0.16

Note: Metal-matrix composites use same data as matrix alloy. Surface area exposed is modified.

Specimens and Procedures

DF Study: The corrosion cell was a modified polarographic trielectrode cell constructed from Teflon.[1,2] The reference electrode in the DF solution was a silver wire in 0.1 M silver nitrate in acetonitrile. The working electrode was an alloy cylinder, 1.2-cm^2 surface area. The counter electrode was a spiralled 40-gauge platinum wire. In order to describe the anodic and cathodic processes, anodic and cathodic polarization measurements were made utilizing the potential sweep method of potentiostatic polarization. The electrode potential was continuously changed at a constant rate of 5000 mV/hr and current was simultaneously recorded. Corrosion rates in mils per year (mpy) were generally determined by extrapolation of the cathodic portion of the polarization curve to the corrosion potential; pitting scans were performed to elucidate mechanisms of passivation or pitting. One hour potential time data were obtained for all alloys in all environments in order to determine the corrosion potentials. In addition, modified polarization specimens of 1.2- to 4.5-cm^2 surface area were exposed for up to 180 days at room temperature to DF-22 vapor by positioning the specimen above DF-22 solution with and without added organic inhibitors.

Decon Study: A Pyrex cell with a volume of one liter was utilized for potentiodynamic scans. The reference electrode was a saturated calomel electrode (SCE) separated by a glass bridge with a vycor tip. The working electrode disc was contained in a polytetrafluorethylene holder and had a surface area of 1.0 cm^2. The electrochemical cell has been described in detail elsewhere.[3] The scan rate was 0.2 mV/sec. Corrosion rates in mpy were also obtained by extrapolation of Tafel slopes to the corrosion potential.

1. TARANTINO, P. A., and DECKER, M. M. *Use of Electrochemical Techniques to Study the Corrosion of Selected Alloys by DF.* U.S. Army Materials Technology Laboratory, CRDC TR 8403, July 1984.
2. ZABIELSKI, C. V., and LEVY, M. *Corrosion on Metals/Alloys in Methylphosphonic Difluoride.* Extended Abstracts, Electrochemical Society v. 347, 1986, p. 86-87.
3. LEVY, M. *Anodic Behavior of Titanium and Commercial Alloys in Sulfuric Acid.* Corrosion, v. 23, no. 8, August 1967, p. 237.

RESULTS AND DISCUSSION

Compatibility with DF

Potential time curves were obtained for Hastelloy B, Hastelloy C, titanium, Al 6061-T6, Ta-10W, Monel, Ta, and 1020 steel in both DF-2 and DF-22 solutions. Generally, equilibrium potentials were obtained within 30 minutes. Except for Hastelloy B and Hastelloy C, which contain chromium and molybdenum, the corrosion potentials of the other metals/alloys were more active; i.e., negative in DF-22, the higher purity solution. The corrosion potential range for the metals/alloys was (+0.71 V to -0.644 V) in DF-2, the 97.1% solution, and (+0.254 V to -1.100 V) in DF-22, the 99.8% solution.

Polarization curves were obtained for these alloys in DF-2 and DF-22 solutions. Although these curves are analyzed in the text, only a few are shown because of space limitations. The curves for Hastelloy B and C, titanium, Al 6061-T6, and 1020 steel are shown in Figure 1. All of the metals/alloys exhibited lower corrosion current densities in DF-22, the higher purity 99.8% solution than in DF-2 (97.1%) solution. Current densities in the passive region were less than 100 $\mu A/cm^2$ (1 x 10^5 nA/cm^2) with the exception of 1020 steel and Hastelloy C. Aluminum 6061-T6 and Ti exhibited extensive passive regions.

Pitting scans for Ta-10W in DF-2 and DF-22 solutions are shown in Figure 2. Pitting of Ta-10W occurred in DF-22 solution but not in DF-2. Although not shown, none of the remaining alloys pitted in DF-2, but pitting of Hastelloy B, Hastelloy C, and Monel was evident in DF-22, the higher purity solution. The chromium content of Hastelloy B and Hastelloy C and the tungsten content in Ta-10W may impart susceptibility to pitting in the DF-22 solution. DF-22 vapor exposure data also shows that Hastelloy B, Hastelloy C, and Ta-10W underwent pitting.

Table 9 shows that the corrosion rates of those metals/alloys in DF-2 were significantly higher than those in DF-22. The impurities in the DF-2 solution cause an increase in the corrosion rate. The 1020 steel had the highest corrosion rate in both solutions. Al 6061-T6, Hastelloy C, and Ta-10W had corrosion rates of <1 mpy in both solutions.

Table 9. CORROSION RATES IN MILS PER YEAR

Alloy	DF-2	DF-22
1020	99.2	17.5
Monel	15.0	1.8^{sp*}
Ta	9.1	<0.1
Ti	3.3	0.2
Hast. B	2.0	2.0^{sp}
Ta-10W	0.8	0.5^{sp}
Al 6061-T6	0.1	<0.1
Hast. C	<0.1	$<0.1^{sp}$

*SP = slight pitting

Polarization curves were obtained for several aluminum alloys in both DF solutions. These curves show that Al 7075-T6, Al 5083, Al 6061-T6, and Al 2090 develop passive regions in both solutions with current densities less than 20 $\mu A/cm^2$.

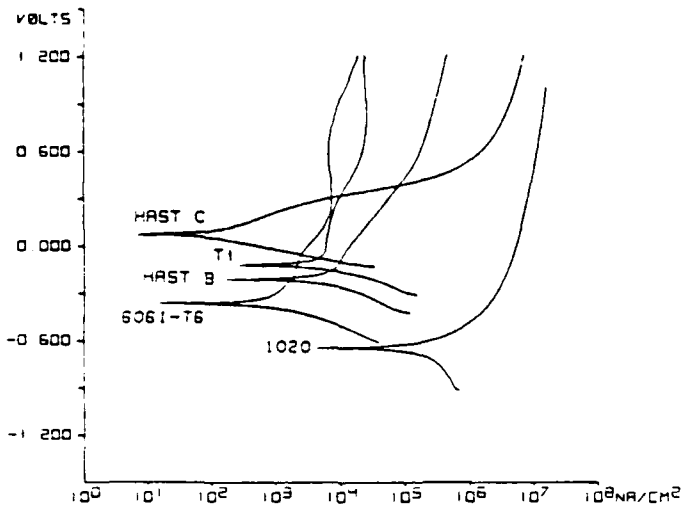

(a) Potentiodynamic Polarization Curves in DF-2 (97.1%) at 25°C, Scan Rate: 1.388 mV/sec

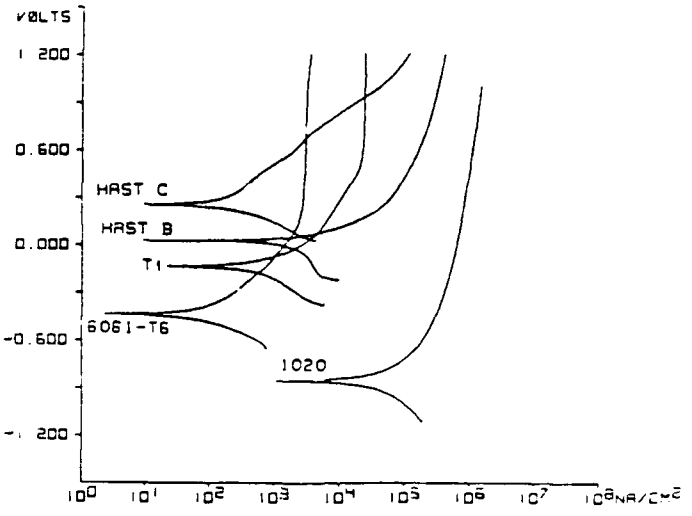

(b) Potentiodynamic Polarization Curves in DF-22 (99.8%) at 25°C, Scan Rate: 1.388 mV/sec

Figure 1.

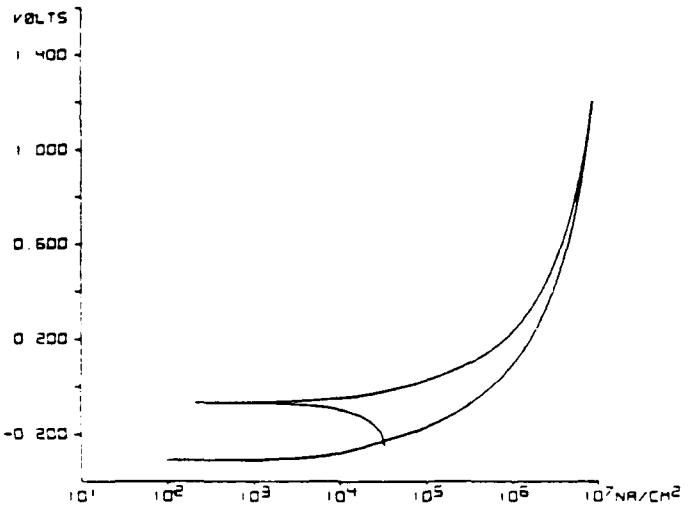

(a) Pitting Scan for Ta-10W in DF-2 at 25°C, Scan Rate: 0.5 mV/sec

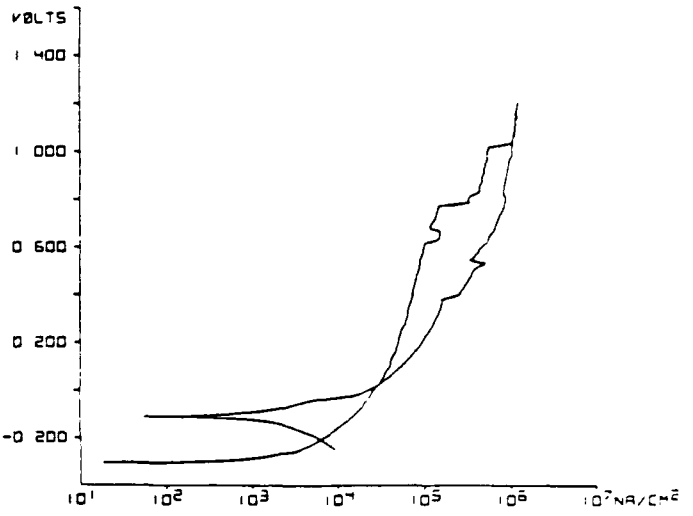

(b) Pitting Scan for Ta-10W in DF-22 at 25°C, Scan Rate: 0.5 mV/sec

Figure 2.

Table 10 lists the corrosion rates determined from the extrapolation of the cathodic and anodic Tafel slopes to the corrosion potential. Aluminum alloys, Al 7075-T6, Al 5083, Al 6061-T6, and Al 2090 have corrosion rates <1 mpy in both DF-2 and DF-22 solutions. The remaining alloys, 4043 and 2017, exhibit slightly higher corrosion rates (<3 mpy). Pitting scan data in Table 10 for the DF-22 solution indicated that Al 5083, which contains 4.5% magnesium, and Al 2090, which contains 2.4% lithium, underwent pitting. Visual examination of the polarization specimens after completion of the pitting scans showed evidence of pitting in Al 5083 and Al 4043. Table 10 also shows that Al 5083 and Al 6061-T6 pit when exposed to DF-22 vapor.

Table 10. POTENTIODYNAMIC CORROSION RATES AND PITTING OBSERVATIONS FOR NONFERROUS ALLOYS IN DF-2 (97.1%) AND DF-22 (99.8%) AT 25°C

	Corrosion Rate (mpy)				Pitting in DF-22		
	DF-2		DF-22		Polarization		Exposure
Alloy	Cathodic	Anodic	Cathodic	Anodic	Scan	Visual	Vapor
Al 7075-T6	0.40	nd	0.06	0.07	N	N	nd
Al 5083	0.42	0.49	0.07	0.07	P	nd	PP
Al 2090	0.49	0.59	0.09	0.08	SP	SP	N
Al 2017	0.04	0.08	0.62	1.39	N	N	nd
Al 6061-T6	0.59	0.39	0.03	0.04	N	nd	PP
Al 4043	3.09	1.11	0.64	1.47	N	HP	N
Pure Cu	67.6	39.22	1.53	1.90	P	PP	nd
Cu (5% Zn)	nd	nd	2.00	2.82	P	nd	nd
Cu (30% Zn)	nd	nd	1.60	1.69	SP	SP	nd
Cu (30% Zn, 2% Pb)	23.64	45.62	0.28	3.06	P	PP	nd
Pure Mg	nd	nd	10.94	16.81	HP	P	HP
U (0.75% Ti) (Warm Worked)	nd	nd	5.01	5.36	SP	N	nd

Key for Pitting Data:

nd = No Data
N = No Pitting
PP = Possible Pitting
SP = Slight Pitting
P = Pitting
HP = Heavy Pitting

Examination of polarization curves for selected copper alloys in both DF-2 (97.1%) and DF-22 (99.8%) solutions showed that copper alloys exhibited lower passive current densities (100 $\mu A/cm^2$) in DF-22 than in DF-2 solution. The addition of zinc to copper displaces the curves toward more negative potentials. The corrosion rates in DF-2 solution for copper and the copper alloy containing 38% Zn, 2% Pb (this alloy was machined from a brass valve used in a one ton GB agent container) listed in Table 10 exceeded 20 mpy, and are significantly higher than those for the copper alloys in DF-22 solution. The corrosion rates in DF-22 solution were between 1.53 and 3.06 mpy, except for Cu (38% Zn, 2% Pb) which had a rate of 0.28 mpy. Pitting scan data in Table 10 for the DF-22 solution disclosed that pitting occurred. Visual examination of the polarization specimens after the completion of the pitting scans confirmed that pitting does indeed occur.

Analysis of the polarization curves for commercially pure magnesium, U-0.75% Ti (warm worked), Al 6061-T6, and Al 2017 in DF-22 solution showed that magnesium and U-0.75% Ti exhibited more active corrosion potentials and higher current densities, but passive current densities did not exceed 100 $\mu A/cm^2$. Passive current densities for the Al alloys were

between 5 and 10 $\mu A/cm^2$. The corrosion rates in DF-22 solution of commercially pure magnesium and U-0.75% Ti significantly exceeded the rates for Al 6061-T6 and Al 2017, but were lower than those for 1020 steel (Tables 10 and 11). Pitting scan data for DF-22 solution indicated severe pitting occurred on commercially pure magnesium, and slight pitting occurred on warm worked U-0.75% Ti. Visual examination of the polarization specimens after completion of the pitting scans confirmed the occurrence of pitting in commercially pure magnesium. DF-22 (99.8%) vapor exposure data also shows severe pitting of magnesium.

Table 11. POTENTIODYNAMIC CORROSION RATES AND PITTING OBSERVATIONS FOR FERROUS AND NICKEL ALLOYS IN DF-2 (97.1%) AND DF-22 (99.8%) AT 25°C

	Corrosion Rate (mpy)				Pitting in DF-22		
	DF-2		DF-22		Polarization		Exposure
Alloy	Cathodic	Anodic	Cathodic	Anodic	Scan	Visual	Vapor
20 Cb3	nd	nd	0.30	0.22	N	N	nd
317L SS	nd	nd	1.20	1.17	N	N	nd
316L SS	36.94	77.00	0.27	0.33	N	PP	N
304 SS	43.47	44.16	0.16	0.24	SP	PP	HP
430 SS	nd	nd	0.73	0.91	PP	SP	nd
1020	98.66	135.90	17.50	20.79	N	nd	N
Hastelloy C	0.19	0.23	0.08	0.05	P	nd	PP
Hastelloy B	2.06	2.24	0.68	1.58	SP	nd	SP
Monel	14.97	36.77	1.81	2.45	PP	nd	nd
Ni 200	nd	nd	2.40	2.58	SP	PP	nd
Commercially Pure Ni	nd	nd	1.38	0.88	P	PP	nd

Key for Pitting Data

nd = No Data
N = No Pitting
PP = Possible Pitting
SP = Slight Pitting
P = Pitting
HP = Heavy Pitting

Polarization curves for stainless and other ferrous alloys in DF-22 (99.8%) solution showed that the higher chromium and nickel content of stainless steels displaced the 1020 steel curve toward more noble potentials and lower current densities. The corrosion rates for 304 SS and 316L SS in DF-2 solution markedly exceeded those in DF-22 solution but were lower than the corrosion rates for 1020 steel. Pitting scan data in Table 11 indicates that slight pitting occurred on 304 SS and 430 SS in the DF-22 solution. Visual examination of polarization specimens after completion of pitting scans disclosed slight pitting for 430 SS, 304 SS, and 316L SS. The DF-22 vapor exposure data in Table 11 indicates severe pitting of 304 SS, but no pitting of 316L SS.

Comparing polarization curves for nickel alloys in DF-22 solution with pure nickel, it appears that the addition of chromium and molybdenum to nickel displaced the curves for Hastelloy B and Hastelloy C toward more noble potentials and lower current densities. The addition of copper to pure nickel shifts the curve for Monel toward more negative or active potentials. The corrosion rates in DF-22 solution, in order of increasing rates, were Hastelloy C (0.08 mpy), Hastelloy B (0.68 mpy), commercially pure nickel (1.38 mpy), Monel (1.81 mpy), and Ni 200 (2.40 mpy). The corrosion rates in DF-2 solution were somewhat higher than in DF-22 for Hastelloy C (0.19 mpy) and Hastelloy B (2.06 mpy), and markedly higher for Monel (14.97 mpy). Pitting scan data in Table 11 indicates that the nickel alloys

Hastelloy C, Hastelloy B, Ni 200, Monel, and commercially pure nickel undergo pitting in the DF-22 solution. The visual examination of polarization specimens after completion of the pitting scans revealed pitting of Ni 200 and commercially pure nickel. DF-22 vapor exposure data in Table 11 indicates pitting of Hastelloy B and Hastelloy C.

Inhibitor Studies

Table 12 lists the percent cathodic and anodic inhibition efficiencies of several organic compounds in reducing the corrosion rate of mild steel in DF-2 solutions. The inhibition is based on corrosion rates determined from cathodic and anodic Tafel slope extrapolations which do not account for pitting. Sulfanilimide was found to have the highest cathodic and anodic inhibiting efficiencies of 74.3 and 84.2%. Benzonitrile, benzothiazole, and benzotriazole additions provided cathodic and anodic inhibiting efficiencies greater than 50%. Sulfanilimide, benzonitrile, and benzotriazole are N-containing additives while benzothiazole is an S-containing additive. These species may chemically absorb on the surface to inhibit corrosion by acidic fluorides (HF) and acidic chlorides (HCl). The remaining organic inhibitor additions NLS (Na salt), NLS (free acid), benzimidazole (N-containing additives), and 2-benzothiazole-ethiol and 1-phenyl-2-thiourea (S-containing additives) had cathodic and anodic inhibiting efficiencies lower than 50%.

Table 12. POTENTIODYNAMIC CORROSION RATES AND PERCENT INHIBITING EFFICIENCIES (I.E.%) OF 1020 STEEL IN DF-2 (97.1%) WITH 0.025 MOLAR ORGANIC INHIBITOR ADDITIONS

	Cathodic		Anodic	
Inhibitor Addition (0.025 M)	MPY	I.E.%	MPY	I.E.%
DF-2	98.7	-	135.9	-
Sulfanilamide	25.4	74.3	21.5	84.2
Benzonitrile	33.7	65.8	42.7	68.6
Benzothiazole	35.9	63.6	50.2	63.1
Benzotriazole	43.5	56.0	63.1	53.6
NLS (Na Salt)*	55.1	44.2	82.7	39.1
NLS (Free Acid)*	55.9	43.4	98.6	27.4
2-Benzothiazolethiol	58.2	41.0	106.5	21.6
Benzimidazole	-	-	117.9	13.2
1-Phenyl-2-Thiourea	71.8	27.2	136.0	0.0

*N-Lauroyl Sarcosine

Table 13 contains similar data for 316L SS. Benzotriazole was found to have the highest cathodic and anodic inhibiting efficiencies of 97.5 and 98.6%, respectively, but pitting scan data and visual examination showed that pitting occurred. Since comparable polarization data and visual examination of 316L SS exposed to DF-2 solution without an inhibitor showed no evidence of pitting, it is clear that benzotriazole will cause pitting of 316L SS despite the excellent inhibition efficiencies displayed. NLS (free acid) gave the next highest cathodic and anodic inhibiting efficiencies of 40.8 and 73.8%, respectively.

Table 13. POTENTIODYNAMIC CORROSION RATES AND PERCENT INHIBITING EFFICIENCIES (I.E.%) OF 316L SS IN DF-2 (97.1%) WITH 0.025 MOLAR ORGANIC INHIBITOR ADDITIONS

	Cathodic		Anodic	
Inhibitor Addition (0.025 M)	MPY	I.E.%	MPY	I.E.%
DF-2	43.5	-	44.2	-
Benzotriazole	1.08	97.5	0.63	98.6
NLS (Free Acid)*	25.7	40.8	11.6	73.8
NLS (Na Salt)*	30.3	30.4	13.9	68.6
Benzothiazole	31.0	28.6	20.5	63.6

*N-Lauroyl Sarcosine

Figure 3 compares anodic polarization curves for 304 SS in DF-22 with and without a 0.025 M benzothiazole addition. The inhibitor addition shifted the curve toward more negative potentials and lower current densities, and reduced the passive current density from 80 $\mu A/cm^2$ to 8 $\mu A/cm^2$. Table 14 compares the efficacy of the four different inhibitors for 304 SS in DF-22. Benzotriazole had the highest cathodic inhibiting efficiency of 76.4% followed by benzothiazole and sulfanilimide (greater than 50%) and the Na-salt of n-lauroyl sarcosine (below 50%). Pitting scan data in Table 14 shows that all the inhibitor additions eliminated pitting. Visual examination of the polarization specimens confirmed the elimination of pitting by the four inhibitors. Figure 4 shows that 304 stainless specimens exposed to the vapor above the DF-22 (99.8%) solution with 0.025 M benzothiazole were free of pitting.

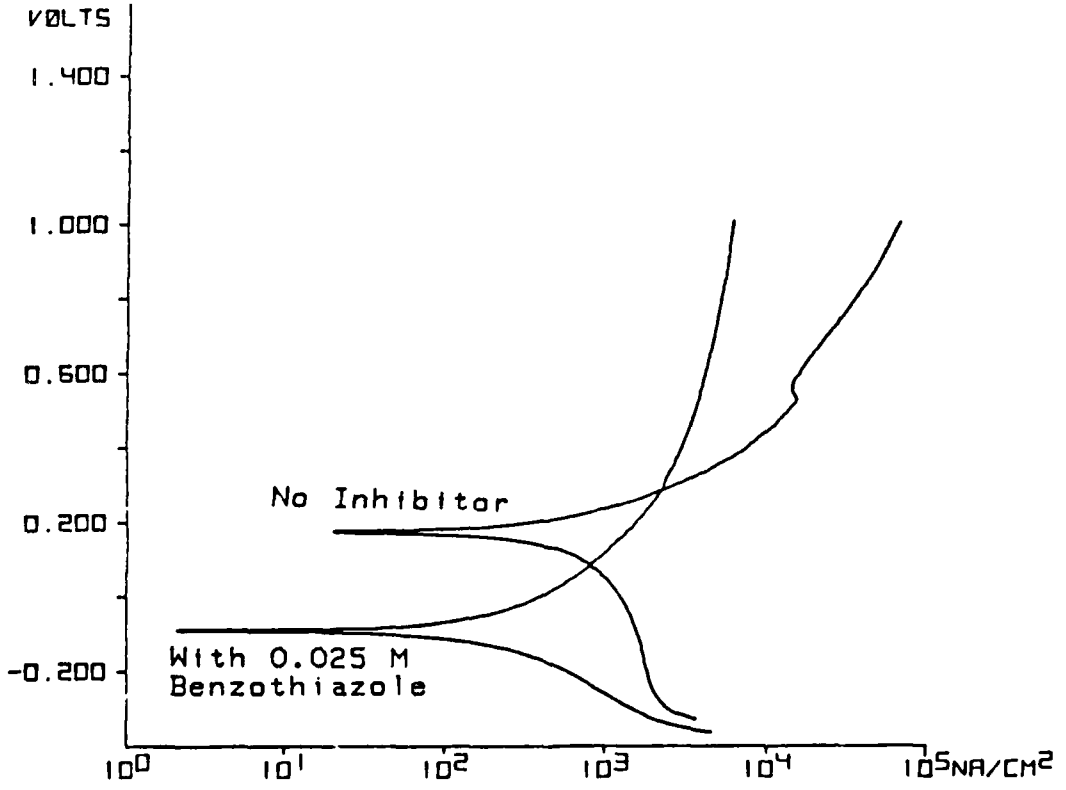

Figure 3. Effect of 0.025 M benzothiazole on potentiodynamic polarization curves for 304 SS in DF-22 (99.8%) at 25°C, scan rate: 1.388 mV/sec.

Table 14. POTENTIODYNAMIC CORROSION RATES AND PERCENT INHIBITING EFFICIENCIES (I.E.%) OF 304 SS IN DF-22 WITH ORGANIC INHIBITORS ADDED

	Inhibitor Efficiency				Pitting Observations			
	Anodic		Cathodic		Polarization		Exposure	
Inhibitor	MPY	I.E.%	MPY	I.E.%	Scan	Visual	Liquid	Vapor
No Inhibitor 0.025 M	0.329	-	0.270	-	SP	PP	HP	HP
Benzotriazole 0.025 M	0.097	70.5	0.064	76.4	N	N	nd	nd
Benzothiazole 0.025 M	0.096	70.8	0.083	69.6	N	N	N	N
Sulfanilamide 0.025 M	0.164	50.2	0.130	52.0	N	N	nd	nd
N-Lauroyl Sarcosine (Na Salt)	0.185	43.8	0.163	39.9	N	N	nd	nd

Key for Pitting Observations:

nd = No Data
N = No Pitting
PP = Possible Pitting
SP = Slight Pittting
P = Pitting
HP = Heavy Pitting

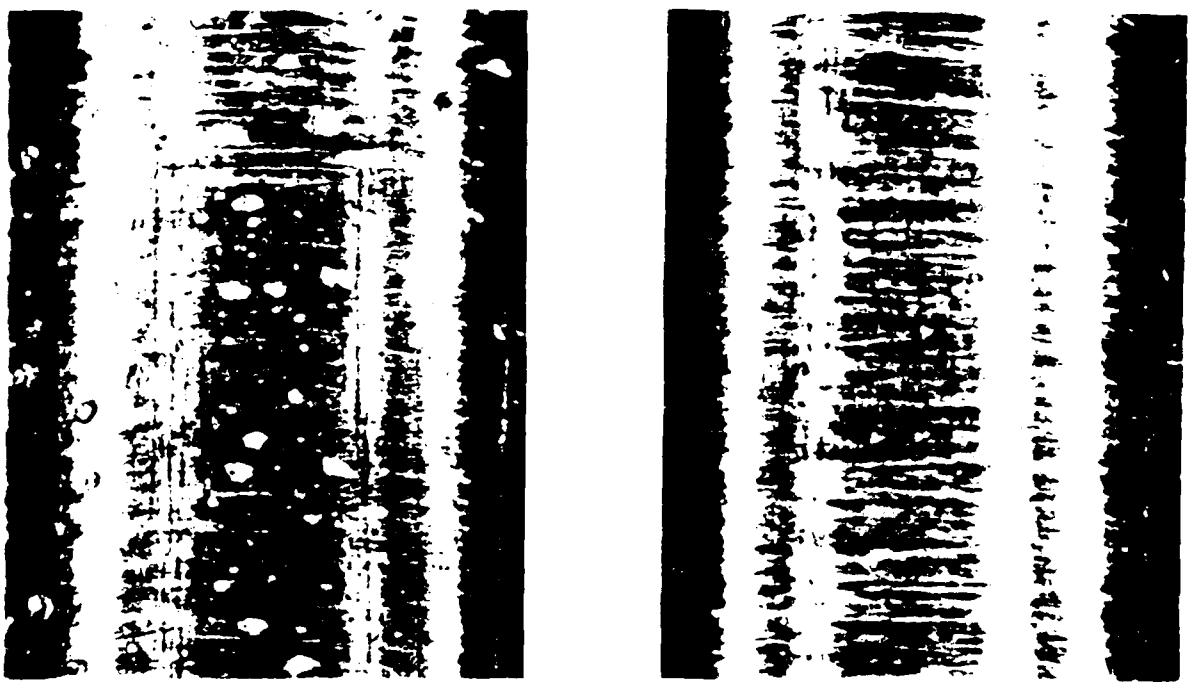

(a) 304 SS in DF-22 Vapor

(b) 304 SS in DF-22 Vapor with 0.025 M Benzothiazole

Figure 4. Elimination of pitting of 304 SS exposed to DF-22 vapor for 30 days by addition of 0.025 M benzothiazole, Mag. 32X.

Figure 5 compares anodic polarization curves for commercially pure magnesium in DF-22 (99.8%) with and without 0.025 M benzothiazole. The addition of the inhibitor shifted the curve toward more noble potentials, showed an active-passive transition, and reduced the critical current for passivity from 100 $\mu A/cm^2$ to 10 $\mu A/cm^2$. Table 15 shows that benzothiazole had a higher cathodic inhibiting efficiency (87.5%) than benzotriazole (71.5%). The pitting

scan data in Table 15 shows that both inhibitors eliminated pitting. Visual examination of the polarization specimens after pitting scans, however, revealed that slight pitting was evident. Figure 6 shows that commercially pure magnesium exposed to DF-22 (99.8%) vapor containing 0.025 M benzothiazole significantly reduces the magnitude of pitting.

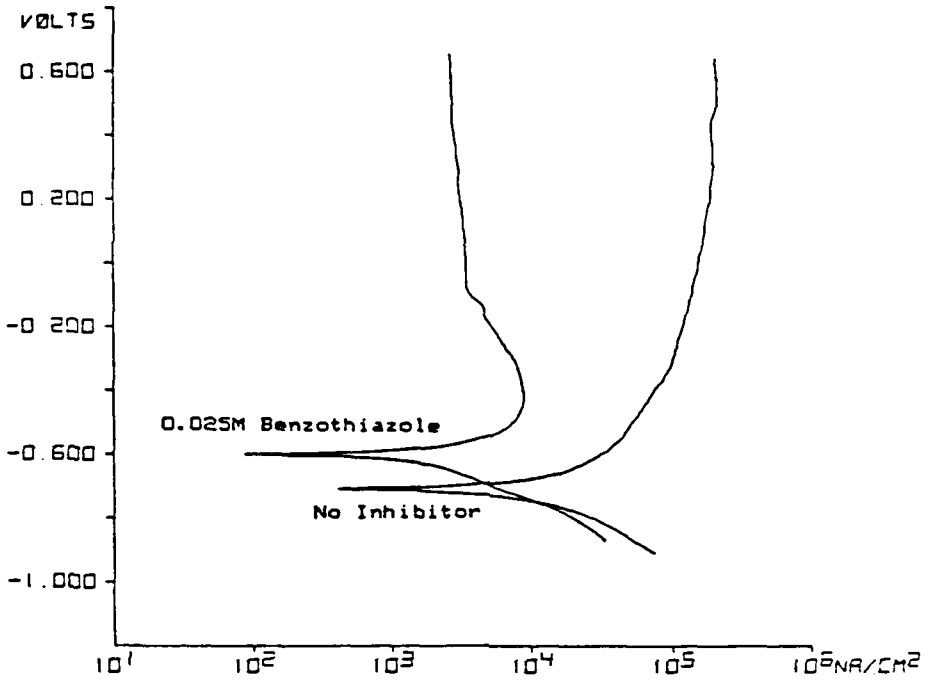

Figure 5. Effect of organic inhibitors on potentiodynamic polarization behavior of commercially pure Mg in DF-22 (99.8%) at 25°C, scan rate: 1.388 mV/sec.

Table 15. POTENTIODYNAMIC CORROSION RATES AND PERCENT INHIBITING EFFICIENCIES (I.E.%) OF COMMERCIALLY PURE Mg IN DF-22 WITH ORGANIC INHIBITORS ADDED

	Inhibitor Efficiency				Pitting Observations		
	Anodic		Cathodic		Polarization		
Inhibitor	*MPY*	*I.E.%*	*MPY*	*I.E.%*	*Scan*	*Visual*	*Vapor*
No Inhibitor 0.025 M	10.94	-	16.81	-	P	HP	HP
Benzothiazole 0.025 M	1.37	87.5	nf	nf	N	SP	P
Benzotriazole 0.025 M	3.09	71.7	3.78	77.5	N	SP	nd

Key for Pitting Observations:

nd = No Data
N = No Pitting
nf = Not Found
SP = Slight Pittting
P = Pitting
HP = Heavy Pitting

(a) Commercially Pure Mg in DF-22 Vapor

(b) Commercially Pure Mg in DF-22 Vapor with 0.025 M Benzothiazole

Figure 6. Reduction of pitting of commercially pure Mg exposed to DF-22 vapor for 15 days by addition of 0.025 M benzothiazole, Mag. 32X.

Compatibility with Decon Agents

Tables 16 through 21 contain corrosion rate data (mpy) for the following alloys and metal-matrix composites: 1020 carbon steel, Carpenter 20Cb3 (a Ni-Cr steel), Ti-6Al-4V (grade 5), aluminum alloys 5083, 6061-T6, 7039, magnesium ZE41A, Al 6061/25 vol% SiC, and magnesium ZE41A/35 vol% FP (fire polished Al_2O_3). These materials were exposed to the following Decon solutions: 10% sodium carbonate solution; 100% DS2, and in dilutions of 50%, 30%, and 20%; a saturated solution of STB as well as a 50% dilution with water.

Table 16 contains corrosion rates in mpy for several alloys exposed to 10% Na_2CO_3 solution. The 1020 carbon steel, stainless steel 20Cb3, and Ti-6Al-4V had low corrosion rates of <1.5 mpy. Current Army armor alloys, Al 5083 and Al 7039, exhibited moderate corrosion rates in excess of 25 mpy. Two recently developed Al-Li alloys, Al 2090 and Al MML 043, had high corrosion rates in excess of 250 mpy. It appears that the copper and lithium alloying constituents in the latter two alloys significantly increased the corrosion rate.

Table 16. ALLOYS IN 10 wt% SODIUM CARBONATE

Alloy	Corrosion Rate (mpy)
C 1020	0.14
Alloy 20Cb3	0.08
Ti-6Al-4V	0.08
Al 5083	28.4
Al 7039	37.4
Al 2090	264.0
Al MML 043	300.0

Tables 17 through 20 list corrosion rates in mpy for additional ferrous alloys, nonferrous alloys, and metal-matrix composites in DS2 solutions. All of the alloys and metal-matrix composites exhibited a low corrosion rate of <0.25 mpy in 100% DS2. When DS2 is diluted with water, the corrosion rate usually increases for all of the alloys and metal-matrix composites. Slight increases were shown for 1020 carbon steel, stainless steel 20Cb3, and Ti-6Al-4V (<1 mpy at all dilutions).

Table 17. FERROUS AND TITANIUM ALLOYS IN DS2

DS2 (vol%)	C 1020 (mpy)	Alloy 20Cb3 (mpy)	Ti-6Al-4V (mpy)
100	0.01	0.03	0.01
50	0.03	0.04	0.04
30	0.20	0.10	0.03
20	0.34	0.25	0.18
0	1.00	0.10	0.02

Table 18. ALUMINUM ALLOYS IN DS2

DS2 (vol%)	Al 5083 (mpy)	Al 7039 (mpy)
100	0.13	0.02
50	180	400
30	490	990
20	360	980
0	0.04	0.08

Table 19. ALUMINUM METAL-MATRIX COMPOSITES IN DS2

DS2 (vol%)	Al 6061 (mpy)	Al 6063[4] (mpy)	Al 6061/SiC (mpy)
100	0.23	0.12	0.22
50	445	421	69
30	>1000	766	444
20	>1000	717	888
0	0.05	7.1	0.24

Table 20. MAGNESIUM METAL-MATRIX COMPOSITES IN DS2

DS2 (vol%)	Mg ZE41A (mpy)	Mg ZE41A/FP (mpy)
100	0.03	0.03
50	0.29	0.48
30	0.24	1.92
20	0.50	0.34
0	4.80	4.90

Aluminum alloys and aluminum metal-matrix composites underwent a significant increase in corrosion rate with dilution reaching a maximum of >300 mpy in the range 20% to 30% DS2. This data is in accord with Tarantino[4] who found that the maximum corrosion rates occurred at 30% DS2. The maximum corrosion rate for the magnesium alloy occurred at 30% DS2. The magnesium alloy ZE41A and metal-matrix composite Mg ZE41A/FP had corrosion rates of <2 mpy for dilutions up to 20% DS2. With further dilutions, the corrosion rate increased to 5 mpy.

Table 21 contains the corrosion rates in mpy for several ferrous alloys, nonferrous alloys, and metal-matrix composites in full strength supertropical bleach (STB) and in 50% dilution. Ti-6Al-4V and Carpenter stainless steel 20Cb3 exhibited corrosion rates below 1.3 mpy in both solutions. Corrosion rates for Al 5083, Al 7039, Al 6061-T6, and Al 6061/SiC were in the range of 10 to 64 mpy with the highest rate achieved by the Al 6061/SiC metal-matrix composite.

Table 21. CORROSION OF ALLOYS IN SUPER TROPICAL BLEACH

Alloy	Full Strength (mpy)	50% Dilution (mpy)
C 1020	156	97
Alloy 20Cb3	1.28	0.28
Ti-6Al-4V	0.14	0.14
Al 5083	10	23
Al 7039	50	20
Al 6061-T6	27	10
Al 6061/SiC	24	64
Mg ZE41A	125	290
Mg ZE41A/FP	330	575

The corrosion rates for 1020 steel in full strength STB and in 50% dilution were higher; 156 and 97 mpy, respectively. The Mg ZE41A and Mg ZE41A/FP had corrosion rates in the range of 125 to 575 mpy in both full strength STB and in 50% dilution. The maximum rate was attained by the Mg ZE41A/FP metal-matrix composite.

4. TARANTINO, P. A., and DAVIS, P. M. *Electrochemical Corrosion Rates of DS2 with Some Aluminum Alloys.* U.S. Army Armament Research and Development Command Technical Report, ARCSL TR 83051, June 1983.

CONCLUSIONS

DF Studies

The corrosion rates of the metals/alloys in 97.1% DF were significantly higher than in 99.8% DF. The Cl, Fe, and other impurities in the 97.1% solution cause an increase in the corrosion rate.

The 1020 steel had the highest corrosion rate in both solutions. Hastelloy C, Ta-10W, Al 6061-T6, Al 5083, Al 2090, and Al 7075-T6 had corrosion rates of <1 mpy in both solutions.

The corrosion potentials of the metals/alloys were generally more active in the higher purity solution except for Hastelloy B, Hastelloy C, 304 SS, and 316L SS, Al 2090, Al 2017, and Cu (38% Zn, 2% Pb).

Pitting tendency as determined from potentiodynamic pitting scans disclosed that pitting did not occur for any metal/alloy in the 97.1% solution, but that pitting did occur in the higher purity 99.8% solution for most alloys.

The best inhibitor for specific alloys in DF is as follows: Sulfanilimide for 1020 steel and benzotriazole for 316L SS in 97.1% DF; benzotriazole for 304 SS and benzothiazole for Mg in 99.8% DF.

Potentiodynamic pitting scans for 304 SS in 99.8% DF solution with 0.025 M additions of benzotriazole, benzothiazole, sulfanilimide, and N-lauroyl sarcosine (Na salt), and for Mg with benzothiazole and benzotriazole additions, showed that these inhibitors reduced or eliminated pitting.

An addition of 0.025 M benzothiazole to the liquid phase greatly reduced the extent of pitting of 304 SS and Mg specimens after long-term exposure to vapor above 99.8% DF.

Decon Studies

Lithium and copper alloying elements significantly increase corrosion rates of aluminum alloys in 10% sodium carbonate solution.

Aluminum alloys and aluminum metal-matrix composites exhibited low corrosion rates in pure DS2, but high corrosion rates (>360 mpy) in the more aggressive dilutions of 20% to 30%. Carbon steel, magnesium alloys, and magnesium metal-matrix composites had significant corrosion rates (>125 mpy) in STB.

The following alloys exhibited low corrosion rates (<2 mpy) in Decon agents: stainless steel 20Cb3 and Ti-6Al-4V in 10% Na_2CO_3; all alloys and metal-matrix composites in 100% DS2; 1020 carbon steel, stainless steel 20Cb3, and Ti-6Al-4V in all dilutions of DS2; Mg ZE41A and Mg ZE41A/FP in dilutions up to 20% DS2; stainless steel Cb3 and Ti-6Al-4V in STB.

The following alloys exhibited moderate corrosion rates (10 to 64 mpy) in Decon agents: Al 5083 and Al 7039 in 10% Na_2CO_3; and Al 5083, Al 7039, Al 6061-T6, and Al 6061/SiC in STB.

ACKNOWLEDGMENT

The methylphosphonic difluoride utilized in this investigation was provided by Pascal A. Tarantino of the U.S. Army Armament, Munitions and Chemical Command, Aberdeen Proving Ground, Maryland 21010.

No. of Copies	To
	Commander, U.S. Army Chemical Research, Development and Engineering Center, Aberdeen Proving Ground, MD 21010-5423
1	ATTN: SMCCR-DDE
1	SMCCR-DDD
1	SMCCR-DDP
1	SMCCR-HV
1	SMCCR-MSI
1	SMCCR-MU
1	SMCCR-MUC
1	SMCCR-MUP
1	SMCCR-NB
1	SMCCR-OPC (B. Eckstein)
1	SMCCR-OPF
1	SMCCR-OPP
1	SMCCR-OPR
1	SMCCR-PPC
1	SMCCR-PPI
1	SMCCR-PPP
1	SMCCR-RS
1	SMCCR-RS (P. A. Tarantino)
2	SMCCR-RSC (E. Penski, W. Shuely)
1	SMCCR-RSL
1	SMCCR-RSP
1	SMCCR-RSP-A (M. Miller)
1	SMCCR-RSP-B
1	SMCCR-RSP-P
1	SMCCR-RSC-P (D. R. Bowie)
1	SMCCR-RSC-P (Dr. K. R. Collins)
1	SMCCR-RST
1	SMCCR-SF
1	SMCCR-SPS-T
1	SMCCR-ST
1	SMCCR-TDT (S. Lawhorne)
1	SMCCR-MUA (Record copy)
	Commandant, U.S. Army Ordnance Missile and Munitions Center and School, Redstone Arsenal, AL 35897-6700
1	ATTN: ATSK-EI (Mr. Cranford)
	Commander, U.S. Army Missile Command, Redstone Scientific Information Center, Redstone Arsenal, AL 35898-5241
1	ATTN: AMSMI-RD-CS-R (Document Section)
	Commander, U.S. Army Missile Command, Redstone Arsenal, AL 35898-5241
1	ATTN: AMSMI-ROC (Dr. B. Fowler)
	Commander, U.S. Army Missile Command, Redstone Arsenal, AL 35898-5500
1	ATTN: AMSMI-RGT (Mr. Maddix)
1	AMSMI-YDL, Bldg. 4505
1	AMSMI-YLP (Mr. N. C. Kattos)
	Commander, Anniston Army Depot, Anniston, AL 36201-5009
1	ATTN: SDSAN-CS
	Commandant, U.S. Army Chemical School, Fort McClellan, AL 36205-5020
1	ATTN: ATZN-CM
1	ATZN-CM-CC
1	ATZN-CM-CS
1	ATZN-CM-CT
1	ATZN-CM-MLB
1	ATZN-CM-NC
	Commander, U.S. Army Aviation Center, Fort Rucker, AL 36362-5000
1	ATTN: ATZQ-CAT-CA-M (CPT P. McCluskey)
1	ATZQ-D-MS
	Commander, U.S. Army Electronic Proving Ground, Fort Huachuca, AZ 85613-7110
1	ATTN: STEEP-DT-F
	Commander, Naval Weapons Center, China Lake, CA 93555
1	ATTN: Code 36
1	Code 366
1	Code 3554
1	Code 3653
1	Code 3656
1	Code 3664
1	Code 3893
1	Code 3917 (Dr. D. V. Houwen) NWC Coordinator

No. of Copies	To
	Commander, U.S. Army Science and Technology Center, Far East Office, San Francisco, CA 96328-5000
1	ATTN: Medical/Chemical Officer
1	AFDPRC/PR, Lowry Air Force Base, CO 80230-5000
1	NORAD/NC CBN, Cheyenne Mountain AFS-STOP 4, Peterson Air Force Base, CO 80914-5601
	Director, Office of Environmental and Life Sciences, Office of the Under Secretary of Defense (R&E), The Pentagon, Washington, DC 20301-3080
1	ATTN: Mr. Thomas R. Dashiell
	Director, Defense Intelligence Agency, Washington, DC 20301-6111
1	ATTN: DT-5A (Mr. C. Clark)
1	HQDA (DAMO-NCC), Washington, DC 20310-0403
1	HQDA (DAMI-FIT-S&T), Washington, DC 20310-1087
1	HQ USAF/INKL, Washington, DC 20330-1550
1	HA AFOSR/NE, Bolling Air Force Base, Washington, DC 20332-6448
	Commander, Naval Air Systems Command, Washington, DC 20361
1	ATTN: PMA 279A (B. Motsuk)
1	PMA 279C (LCDR F. Smartt)
	Commander, Naval Sea Systems Command, Washington, DC 20362-5101
1	ATTN: Code 55X25
	Commander, Naval Sea Systems Command, Theater of Nuclear Warfare Program Office, Washington, DC 20362-5101
1	ATTN: Code TN20A (Dr. G. Patton)
	Commander, Naval Medical Command, Washington, DC 20372-5120
1	ATTN: MEDCOM-02C
	Commander, Naval Research Laboratory, 4555 Overlook Avenue, SW, Washington, DC 20375-5000
1	ATTN: Code 2526 (Library)
1	Code 6182 (Dr. R. Taylor)
	Commanding Officer, Navy Intelligence Support Center, Washington, DC 20390
1	ATTN: NISC-633 (Collateral Library)
	Commanding General, Marine Corps Research, Development and Acquisition Command, Washington, DC 20380-0001
1	ATTN: Code SSC NBC
1	Toxicology Information Center, JH, 652, National Research Council, 2101 Constitution Avenue, NW, Washington, DC 20418
1	OSU Field Office, P.O. Box 1925, Eglin Air Force Base, FL 32542-1925
	Headquarters, Eglin Air Force Base, FL 32542-6008
1	ATTN: AD/YQO/YQX
1	USAFTAWC/THLO
1	AD/YN
1	Mr. L. Rodgers
	Commandant, U.S. Army Infantry School, Fort Benning, GA 31905-5410
1	ATTN: ATSH-CD-CS-CS
	Commander, U.S. Army Infantry Center, Fort Benning, GA 31905-5273
1	ATTN: NBC Branch, Directorate of Plans and Training, Bldg. 2294
	Commandant, U.S. Army Infantry School, Fort Benning, GA 31905-5410
1	ATTN: ATSH-B, NBC Branch
	Commandant, U.S. Army Infantry School, Fort Benning, GA 31905-5800
1	ATTN: ATSH-CD-MLS-C

No. of Copies	To
	Commander, U.S. Army Armament, Munitions and Chemical Command, Rock Island, IL 61299-6000
1	ATTN: AMSMC-ASN
1	AMSMC-IMP-L
1	AMSMC-IRA
1	AMSMC-IRD-T
1	AMSMC-SFS
1	AMSMC-QAS-N (Gloria Aldridge)
	Director, U.S. Army Materiel Command Field Safety Activity, Charlestown, IN 47111-9669
1	ATTN: AMXOS-SE (Mr. W. P. Yutmeyer)
	Commander, Naval Weapons Support Center, Crane, IN 47522-47522-5050
1	ATTN: Code 5063 (Dr. J.R. Kennedy)
	Commander, U.S. Army TRADOC Independent Evaluation Directorate, Fort Leavenworth, KS 66027-5130
1	ATTN: ATZL-TIE-C (Mr. C. Annett)
	Commander, U.S. Army Combined Arms Center, Development Activity, Fort Leavenworth, KS 66027-5300
1	ATTN: ATZL-CAM-M
	Commander, U.S. Army Armor School, Fort Knox, KY 40121-5211
1	ATTN: ATZK-DPT (NBC School)
	Commander, U.S. Army Natick Research, Development, and Engineering Center, Natick, MA 01760-5015
1	ATTN: STRNC-AC
1	STRNC-UE
1	STRNC-WTS
1	STRNC-WT
1	STRNC-IC
1	STRNC-ICC
1	STRNC-IP
1	STRNC-ITP (Mr. Tassinari)
1	STRNC-YB
1	STRNC-YE
1	STRNC-YM
1	STRNC-YS
	Headquarters, Andrews Air Force Base, MD 20334-5000
1	ATTN: AFSC/SDTS
1	AFSC/SGB
	Commanding Officer, Naval Explosive Ordnance Disposal Technology Center, Indian Head, MD 20640-5070
1	ATTN: Code BC-2
1	Commander, Detachment S, USAOG, Team III, Fort Meade, MD 20755-5985
	Commander, Harry Diamond Laboratories, 2800 Powder Mill Road, Adelphi, MD 20783-1145
1	ATTN: DELHD-RT-CB (Dr. Sztankay)
	Commander, U.S. Army Laboratory Command, 2800 Powder Mill Road, Adelphi, MD 20783-1145
2	ATTN: Technical Library
	Director, U.S. Army Concepts Analysis Agency, 8120 Woodmont Avenue, Bethesda, MD 20814-2797
1	ATTN: CSCA-RQL (Dr. Helmbold)
	Director, U.S. Army Human Engineering Laboratory, Aberdeen Proving Ground, MD 21005-5001
1	ATTN: AMXHE-IS (Mr. Harrah)
	Project Manager, Smoke/Obscurants, Aberdeen Proving Ground, MD 21005-5001
2	ATTN: AMCPM-SMK-E (A. Van de Wal)
1	AMCPM-SMK-T
	Commander, U.S. Army Test and Evaluation Command, Aberdeen Proving Ground, MD 21005-5055
1	ATTN: AMSTE-TE-F
1	AMSTE-TE-T
	Director, U.S. Army Ballistic Research Laboratory, Aberdeen Proving Ground, MD 21005-5066
1	ATTN: SLCBR-OD-ST (Tech Reports)

No. of Copies	To
	Director, U.S. Army Materiel Systems Analysis Activity, Aberdeen Proving Ground, MD 21005-5071
1	ATTN: AMXSY-CR (Mrs. F. Liu)
1	AMXSY-GC (Mr. F. Campbell)
1	AMXSY-MP (Mr. H. Cohen)
	Commander, U.S. Army Toxic and Hazardous Materials Agency, Aberdeen Proving Ground, MD 21010-5401
1	ATTN: AMXTH-ES
1	AMXTH-TE
	Commander, U.S. Army Environmental Hygiene Agency, Aberdeen Proving Ground, MD 21010-5422
1	ATTN: HSHB-O/Editorial Office
	Commander, U.S. Army Armament, Munitions and Chemical Command, Aberdeen Proving Ground, MD 21010-5423
1	ATTN: AMSMC-HO (A) (Mr. J. K. Smart)
1	AMSMC-QAC (A)
1	AMSMC-QAE (A)
	Commander, U.S. Army Technical Escort Unit, Aberdeen Proving Ground, MD 21010-5423
1	ATTN: AMCTE-AD
	Commander, U.S. Army Medical Research Institute of Chemical Defense, Aberdeen Proving Ground, MD 21010-5425
1	ATTN: SGRD-UV-L
	Director, Armed Forces Medical Intelligence Center, Building 1607, Fort Detrick, Frederick, MD 21701-5004
1	ATTN: AFMIC-IS
	Commander, U.S. Army Medical Bioengineering Research and Development Laboratory, Fort Detrick, Frederick, MD 21701-5010
1	ATTN: SGRB-UBG (Mr. Eaton)
1	SGRS-UBG-AL, Bldg. 568
	Commander, HQ 1/163d ACR, MT ARNG, P.O. Box 1336, Billings, MT 59103-1336
1	ATTN: NBC (SFC W. G. Payne)
	Director, U.S. Army Research Office, P.O. Box 12211, Research Triangle Park, NC 27709-2211
1	ATTN: SLCRO-CB (Dr. R. Chirardelli)
1	SLCRO-CS
	Commander, U.S. Army Cold Regions Research and Engineering Laboratory, Hanover, NH 03755-1290
1	ATTN: CRREL-RG
	Commander, U.S. Army Production Base Modernization Activity Dover, NJ 07801
1	ATTN: AMSMC-PBE-C(D)/Regber
	Commander, U.S. Army Armament, Research, Development, and Engineering Center, Picatinny Arsenal, NJ 07806-5000
1	ATTN: SMCAR-A-E (S. Morrow)
1	SMCAR-AE (R. A. Trifiletti)
1	SMCAR-CCT
1	SMCAR-FSF-B
1	SMCAR-MSI
1	SMCAR-AET (Bldg. 335)
	Project Manager, Cannon Artillery Weapons Systems, Picatinny Arsenal, NJ 07806-5000
1	ATTN: AMCPM-CAWS-A
	Director, Los Alamos National Laboratory, Los Alamos, NM 87545
1	ATTN: T-DOT MS P371 (S. Gerstl)
	Commander/Director, U.S. Army Atmospheric Sciences Laboratory, White Sands Missile Range, NM 88002-5501
1	ATTN: SLCAS-AE (Dr. F. Niles)
1	SLCAS-AE-E (Dr. D. Snider)
1	SLCAS-AR (Dr. E. M. Holt)
1	SLCAS-AR-A (Dr. M. Heaps)
1	SLCAR-AR-P (Dr. C. Bruce)
1	SLCAR-AR-M (Dr. R. Sutherland)

No. of Copies	To
	Director, U.S. Army TRADOC Analysis Command, White Sands Missile Range, NM 88002-5502
1	ATTN: ATOR-TSL
1	ATOR-TDB (L. Dominquez)
	Commander, U.S. Army Scientific and Technical Information Team, Europe, Box 48, APO New York 09079-4734
1	ATTN: AMXMI-E-CO
	Commander, Headquarters, 3d Ordnance Battalion, APO New York 09189-2737
1	ATTN: AEUSA-UH
	Commander, U.S. Military Academy, Department of Physics, West Point, NY 10996-1790
1	ATTN: MAJ Decker
	Headquarters, Wright Patterson Air Force Base, OH 45433-6503
1	ATTN: AFWAL/FIEEC
1	ASD/AESD
1	AAMRL/HET
1	FTD-TQTR, Wright Patterson Air Force Base, OH 45433-6508
1	AFWAL/FIES/SURVIAC, Wright Patterson Air Force Base, OH 45433-6553
1	AAMRL/TID, Wright Patterson Air Force Base, OH 45433-6573
	Commandant, U.S. Army Field Artillery School, Fort Sill, OK 73503-5600
1	ATTN: ATSF-GA
	Commander, Naval Air Development Center, Warminster, PA 18974-5000
1	ATTN: Code 60332 (D. Herbert)
	Commandant, U.S. Army Academy of Health Sciences, Fort Sam Houston, TX 78234-6100
1	ATTN: HSHA-CDH (Dr. R. H. Mosebar)
1	HSHA-CDS (CPT Eng)
1	HSHA-IPM
	Headquarters, Brooks Air Force Base, TX 78235-5000
1	ATTN: HSD/RDTK
1	HSD/RDS
1	USAFSAM/VNC
	Commander, U.S. Army Dugway Proving Ground, Dugway, UT 84022-5010
1	ATTN: STEDP-SD (Dr. L. Salomon)
	Commander, U.S. Army Dugway Proving Ground, Dugway, UT 84022-6630
1	ATTN: STEDP-SD-TA-F (Technical Library)
	HQ, Ogden Air Material Area, Hill Air Force Base, UT 84056-5609
1	ATTN: MMWM
	Director, U.S. Army Communications-Electronics Command, Night Vision and Electro-Optics Directorate, Fort Belvoir, VA 22060-5677
1	ATTN: AMSEL-NV-D (Dr. R. Buser)
	Commander, Marine Corps Development and Education Command, Quantico, VA 22134-5080
1	ATTN: Code D091, SPWT Section
	Deputy Director, Marine Corps Institute, Arlington, VA 22222-0001
1	ATTN: NBC CD; CDD2
	Commander, U.S. Army Nuclear and Chemical Agency, 7500 Backlick Road, Bldg. 2073, Springfield, VA 22150-3198
1	ATTN: MONA-CM
	Chief of Naval Research, 800 N. Quincy Street, Arlington, VA 22217
1	ATTN: Code 441

No. of Copies	To
	Commander, U.S. Army Materiel Command, 5001 Eisenhower Avenue, Alexandria, VA 22333-0001
1	ATTN: AMCCN
1	AMCSF-C
1	AMCLD
1	Dr. Richard Chait
1	S. J. Lorber
	Commander, Defense Technical Information Center, Cameron Station, Bldg. 5, 5010 Duke Street, Alexandria, VA 22304-1145
2	ATTN: DTIC-FDAC
	Commander, Naval Surface Weapons Center, Dahlgren, VA 22448
1	ATTN: Code E431
1	Code G51 (Brumfield)
	Commander, U.S. Army Foreign Science and Technology Center 220 Seventh Street, NE, Charlottesville, VA 22901-5396
1	ATTN: AIAST-CW2
	Director, Aviation Applied Technology Directorate, Fort Eustis, VA 23604-5577
1	ATTN: SAVRT-ATL-ASV
	Commander, U.S. Army Training and Doctrine Command, Fort Monroe, VA 23651-5000
1	ATTN: ATCD-N
1	HQ TAC/DRPS, Langley Air Force Base, VA 23665-5001
	Commander, U.S. Army Logistics Center, Fort Lee, VA 23801-6000
1	ATTN: ATCL-MCF
	Commander, U.S. Army Logistics Center, Fort Lee, VA 23801-6000
1	ATTN: ATCL-MCF
	U.S. Army Depot System Command, Chambersburg, PA 17201
1	ATTN: Library
	Commander, Anniston Army Depot, Anniston, AL 36202
1	ATTN: SDSAN-QA
	Commander, Lexington-Bluegrass Army Depot, Lexington, KY 40507
1	ATTN: SDSLX-QA
	Commander, Pueblo Army Depot, Pueblo, CO 81001
1	ATTN: SDSTE-PU-Q
	Commander, Tooele Army Depot, Tooele, UT 84074
1	ATTN: SDSTE-QA
	Commander, Umatilla Army Depot, Hermiston, OR 97838
1	ATTN: Library
	U.S. Army Materials Technology Laboratory, Watertown, MA 02172-0001
2	ATTN: SLCMT-TML
1	Author

U.S. Army Materials Technology Laboratory
Watertown, Massachusetts 02172-0001
CORROSION AND CORROSION INHIBITION OF METALS/ALLOYS IN METHYLPHOSPHONIC DIFLUORIDE AND DECONTAMINATING SOLUTIONS - Chester V. Zabielski, Milton Levy, and James Scanlon

Technical Report MTL TR 89-61, July 1989, 20 pp-illus-tables

AD ________
UNCLASSIFIED
UNLIMITED DISTRIBUTION

Key Words

Corrosion-resistant alloys
Corrosion inhibition
Decontamination materials

Electrochemical potentiodynamic polarization studies have been carried out for a variety of ferrous and nonferrous metals in methylphosphonic difluoride. Studies of the effect of organic inhibitors on the corrosion rate of 1020 steel, 316 and 304 stainless steel and magnesium in methylphosphonic difluoride were also carried out. In addition, electrochemical studies were conducted in Decon solutions of sodium carbonate, DS2, and STB. General corrosion rates are reported for ferrous alloys, titanium, aluminum alloys, magnesium, and two metal-matrix composites in full strength and diluted Decon solutions.

U.S. Army Materials Technology Laboratory
Watertown, Massachusetts 02172-0001
CORROSION AND CORROSION INHIBITION OF METALS/ALLOYS IN METHYLPHOSPHONIC DIFLUORIDE AND DECONTAMINATING SOLUTIONS - Chester V. Zabielski, Milton Levy, and James Scanlon

Technical Report MTL TR 89-61, July 1989, 20 pp-illus-tables

AD ________
UNCLASSIFIED
UNLIMITED DISTRIBUTION

Key Words

Corrosion-resistant alloys
Corrosion inhibition
Decontamination materials

Electrochemical potentiodynamic polarization studies have been carried out for a variety of ferrous and nonferrous metals in methylphosphonic difluoride. Studies of the effect of organic inhibitors on the corrosion rate of 1020 steel, 316 and 304 stainless steel and magnesium in methylphosphonic difluoride were also carried out. In addition, electrochemical studies were conducted in Decon solutions of sodium carbonate, DS2, and STB. General corrosion rates are reported for ferrous alloys, titanium, aluminum alloys, magnesium, and two metal-matrix composites in full strength and diluted Decon solutions.

U.S. Army Materials Technology Laboratory
Watertown, Massachusetts 02172-0001
CORROSION AND CORROSION INHIBITION OF METALS/ALLOYS IN METHYLPHOSPHONIC DIFLUORIDE AND DECONTAMINATING SOLUTIONS - Chester V. Zabielski, Milton Levy, and James Scanlon

Technical Report MTL TR 89-61, July 1989, 20 pp-illus-tables

AD ________
UNCLASSIFIED
UNLIMITED DISTRIBUTION

Key Words

Corrosion-resistant alloys
Corrosion inhibition
Decontamination materials

Electrochemical potentiodynamic polarization studies have been carried out for a variety of ferrous and nonferrous metals in methylphosphonic difluoride. Studies of the effect of organic inhibitors on the corrosion rate of 1020 steel, 316 and 304 stainless steel and magnesium in methylphosphonic difluoride were also carried out. In addition, electrochemical studies were conducted in Decon solutions of sodium carbonate, DS2, and STB. General corrosion rates are reported for ferrous alloys, titanium, aluminum alloys, magnesium, and two metal-matrix composites in full strength and diluted Decon solutions.

U.S. Army Materials Technology Laboratory
Watertown, Massachusetts 02172-0001
CORROSION AND CORROSION INHIBITION OF METALS/ALLOYS IN METHYLPHOSPHONIC DIFLUORIDE AND DECONTAMINATING SOLUTIONS - Chester V. Zabielski, Milton Levy, and James Scanlon

Technical Report MTL TR 89-61, July 1989, 20 pp-illus-tables

AD ________
UNCLASSIFIED
UNLIMITED DISTRIBUTION

Key Words

Corrosion-resistant alloys
Corrosion inhibition
Decontamination materials

Electrochemical potentiodynamic polarization studies have been carried out for a variety of ferrous and nonferrous metals in methylphosphonic difluoride. Studies of the effect of organic inhibitors on the corrosion rate of 1020 steel, 316 and 304 stainless steel and magnesium in methylphosphonic difluoride were also carried out. In addition, electrochemical studies were conducted in Decon solutions of sodium carbonate, DS2, and STB. General corrosion rates are reported for ferrous alloys, titanium, aluminum alloys, magnesium, and two metal-matrix composites in full strength and diluted Decon solutions.